b-flavour tagging in pp collisions

Alex Birnkraut[*]

TU Dortmund

E-mail: a.birnkraut@cern.ch

In the system of neutral B mesons CP-violation and meson mixing can be measured using time-dependent analyses, as performed at the LHCb experiment. For such analyses the knowledge of the flavour of the mesons at production is mandatory. This information is provided by "flavour tagging" techniques. A description of the flavour tagging algorithms used at the LHCb experiment during Run I in pp collisions at $\sqrt{s} = 7,8\,\mathrm{TeV}$ is reported.

---

[*]Speaker.

1. Introduction

The aim of the Flavour Tagging algorithms is to determine the flavour of neutral B mesons at their production. These algorithms are called taggers and can be classified in two groups. The same side (SS) taggers use charged particles which are created in the fragmentation process of the signal b quark. The opposite side (OS) taggers infer the flavour of the non-signal b quark of the $b\bar{b}$ pair produced in the pp collision by looking e.g. for leptons originating from semileptonic $b \to cW$ transitions or kaons coming from $b \to c \to s$ transitions (Figure 1) [1].

The performance of the Flavour Tagging algorithms is characterised by the tagging efficiency

$$\varepsilon_{\text{tag}} = \frac{N_{\text{right}} + N_{\text{wrong}}}{N_{\text{all}}}, \tag{1.1}$$

the probability of the tagging decision to be wrong

$$\omega = \frac{N_{\text{wrong}}}{N_{\text{right}} + N_{\text{wrong}}} \tag{1.2}$$

and the dilution $D = 1 - 2\omega$. The quantities N_{right}, N_{wrong} and N_{all} are the numbers of the right tagged, wrong tagged, and all candidates respectively, i.e. tagged and untagged candidates.

Each tagger provides a per-event tag decision d and a probability η of the decision to be wrong. This predicted mistag probability η is calibrated on data with a function $\omega(\eta)$. Weighting each signal candidate with $D = 1 - 2\omega(\eta)$ leads to an corrected per-event dilution factor. The statistical power of a *CP* or mixing asymmetry measurement using tagging algorithms is proportional to the effective tagging efficiency

$$\varepsilon_{\text{eff}} = \varepsilon_{\text{tag}} \frac{1}{N_{\text{tag}}} \sum_{i=1}^{N_{\text{tag}}} (1 - 2\omega_i(\eta))^2. \tag{1.3}$$

Thus any improvement to this effective tagging efficiency increases the statistical power of time dependent measurements using flavour tagging.
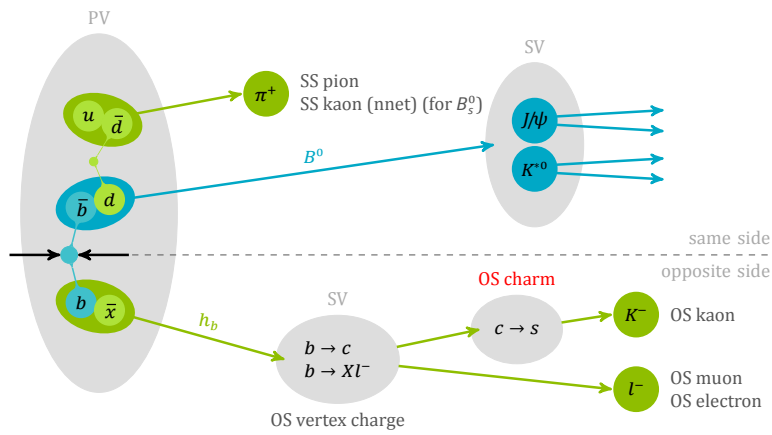

Figure 1: Scheme of the different flavour tagging algorithms. Same side taggers are shown in the upper part, opposite side taggers in the lower part.

2. Flavour Tagging algorithms at LHCb

For the opposite side tagging algorithms there are mainly two different types of algorithms. Single particle taggers identify electrons, muons and kaons coming from the other b hadron. To select these particles a large impact parameter significance with respect to the primary vertex and a large transverse momentum p_T are required. For particle identification requirements on the difference between the logarithm of the likelihood for the muon, electron, kaon or proton and the pion hypothesis are applied. In case of multiple candidates from one tagging algorithm the candidate with the highest transverse momentum is chosen.

In contrast to this method the OS vertex charge tagger does not use single tracks but a weighted charge of a secondary vertex to take a tag decision. The secondary vertex is reconstructed from two tracks which have the highest probablity to originate from the OS b hadron. From this seed more tracks that are compatible with coming from the secondary vertex but not from the primary vertex are added to the vertex to form the final $b$hadron candidate. Finally a weighted charge is calculated as a sum of the charges Q_i of all tracks associated to the vertex

$$Q_{\text{vtx}} = \frac{\sum_i p_T^k(i) Q_i}{\sum_i p_T^k(i)}, \tag{2.1}$$

weighted by their transverse momentum p_T to the power k. The value k optimises the effective tagging efficiency.

For the same side tagging one has to distinguish between B_d^0 and B_s^0 mesons as the accompanying quark is a d or a s quark, respectively. In case of a B_d^0 meson an additional charged pion from the d quark, which can hadronise with an u quark, emerges. Also pions from excited states as B^* and B^{**} have the same charge as pions from the direct fragmenation process with a B^0 meson. Therefore the pion candidates are required to be charged particles with high momentum and transverse momentum originating from the primary vertex [11]. If the signal B meson is a B_s^0, a kaon can be formed from the additional s quark and an u quark.

2.1 SS kaon tagging using neural nets (NN)

The first version of the SS kaon tagger developed at the LHCb experiment uses a selection based on a sequential set of requirements on some discriminating variables to identify the tagging kaon and a neural net (NN) to estimate the mistag probabilty η. An updated version of this tagger, the SS kaon neural net tagger, uses two NN. The first NN distinguishes between fragmentation tracks and the underlying event tracks (see figure 2.1). The fragmentation tracks are the signal tracks for the SS kaon tagger, i.e. the tracks are the searched tagging particle tracks [2]. The second NN assigns the final tag and mistag [3].

Compared to the "cut-based" SS kaon, the SS kaon NN gives a relative improvement of 50 % (41 %) in ε_{eff} for $B_s^0 \to D_s^- \pi^+$ ($B_s^0 \to J/\psi\phi$). This improvements can be observed also when comparing the effective tagging efficiencies in the measurements of ϕ_s at LHCb. The effective tagging efficiencies ε_{eff} for the *CP* analyses in $B_s^0 \to J/\psi K^+ K^-$, $\bar{B}_s^0 \to J/\psi \pi^+ \pi^-$ and $\bar{B}_s^0 \to D_s^+ D_s^-$ are listed in table 2.1.
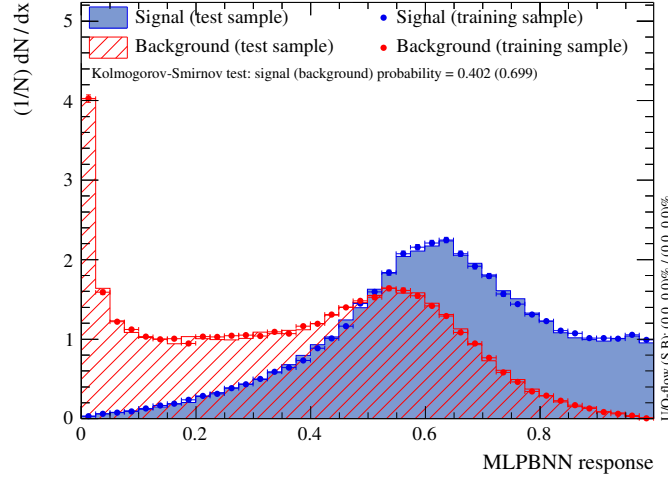
Figure 2: Distribution of NN response for fragmentation tracks (signal) and underlying event tracks (background) [2]

Decay mode	ε_{eff} (1 fb^{-1})	ε_{eff} (3 fb^{-1})
$B_s^0 \to J/\psi K^+ K^-$	3.13 % [4]	3.73 % [5]
$\bar{B}_s^0 \to J/\psi \pi^+ \pi^-$	2.43 % [6]	3.89 % [7]
$\bar{B}_s^0 \to D_s^+ D_s^-$	-	5.33 % [8]

Table 1: Effective tagging efficiencies of the combination of the OS taggers and the SS kaon tagger for the *CP* analyses measuring ϕ_s. In the analyses on 1 fb^{-1} the cut-based version of the SS kaon was used, the analyses on the whole Run I dataset with 3 fb^{-1} used the neural net based version.

2.2 OS charm tagger

A novel tagger introduced at the end of Run I is the OS charm tagger. It uses charm hadrons from the decay chain $b \to c$ from the opposite side b quark to tag the initial flavour. The reconstructed D modes related to the OS b decay are listed in table 2.2. For each mode one boosted

Decay mode	Relative ε_{tag}	Relative ε_{eff}
$D^0 \to K^- \pi^+$	10.0 %	24.0 %
$D^0 \to K^- \pi^+ \pi^+ \pi^-$	5.9 %	8.4 %
$D^+ \to K^- \pi^+ \pi^+$	10.3 %	2.6 %
$D^0, D^+ \to K^- \pi^+ X$	69.7 %	61.5 %
$D^0, D^+ \to K^- e^+ X$	0.5 %	0.2 %
$D^0, D^+ \to K^- \mu^+ X$	3.4 %	0.3 %
$\Lambda_c^+ \to p^+ K^- \pi^+$	0.2 %	2.4 %

Table 2: D meson decay modes with their relative contributions to ε_{tag} and ε_{eff} which are used by the OS charm tagger.

decision tree is used to calculate the mistag probybility η and then the candidate with the best prediction is picked [9]. The OS charm tagger provides a relatively clean measure of the *B* flavour,

63 i.e. it provides low values of η. Depending on the decay mode its stand-alone effective tagging
64 efficiency is between 0.30 % and 0.40 % [9].

3. Calibration of the Flavour Tagging

66   The mistag estimate η provided by the different tagging algorithms has to be corrected and
67 transformed into the true mistag probabilty ω. This is done with a linear calibration function

$$\omega(\eta) = p_0 + p_1 (\eta - \langle \eta \rangle) \tag{3.1}$$

68 where $\langle \eta \rangle$ is the mean mistag estimate. The parameters p_0 and p_1 of this calibration function are
69 extracted in to different ways. Using charged decay modes as $B^+ \to J/\psi K^+$ and $B^+ \to D^0 \pi^+$ the
70 true mistag ω can be extracted by comparing the tag decision with the charge of the kaon or pion
71 in the final state. In neutral decay modes as $B^0 \to J/\psi K^{*0}$, $B^0 \to D^{*-} \mu^+ \nu_\mu$ or $B_s^0 \to D_s^- \pi^+$ a full
72 time-dependent analysis is needed to extract omega from the mixing asymmetry:

$$A_{\text{mix}}(t) \propto (1 - 2\omega) \cos\left(\Delta m_{d/s} t\right) \tag{3.2}$$

73 In both cases the calculation of ω is done in bins of the mistag estimate η and the linear function
74 3.1 is fitted to the (ω, η) pairs. Figure 3 shows the time dependent mixing asymmetry of equation
75 3.2 in the case of the $B^0 \to J/\psi K^{*0}$ decay and the linear calibration function resulting from the fit
76 of all the bins in η.

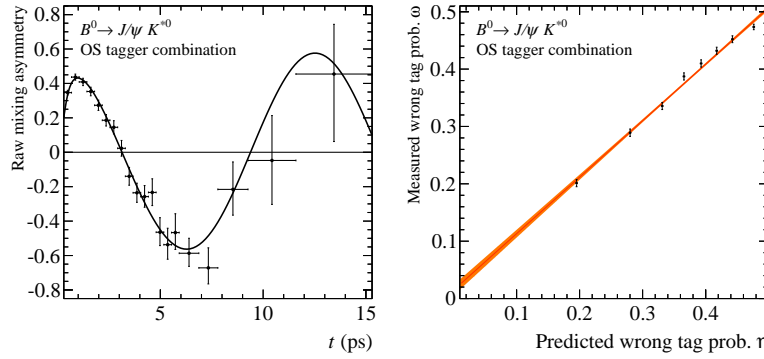In time-dependent analyses of neutral b mesons, systematic uncertainties coming from the Flavour

Figure 3: Overall mixing asymmetry (left) and resulting calibration function (right) for the OS tagger combination in the calibration mode $B^0 \to J/\psi K^{*0}$.

77
78 Tagging are assigned for the uncertainties associated with the calibration method and for the porta-
79 bility of the calibration from the control to the signal decay mode as the calibration depends on
80 the kinematics of the control decay. Adding these two categories of systematic uncertainties, the
81 size of the systematic uncertainty is of the order of the size of the statistical uncertainty on the
82 calibration. For most analyses during Run I the systematic uncertainties are much smaller than the
83 statistical uncertainties. Therefore for most analyses one calibration per tagger valid for all signal
84 channels, taking into account the differences between all control channels, is provided.

For analyses with systematic uncertainties of the order of the statistical uncertainties and the systematic uncertainties are dominated by the uncertainties from the flavour tagging calibration an "ad-hoc" calibration using the best-suited control channel for the analyses is performed.

3.1 *CP* violation in $B^0 \rightarrow J/\psi K_s^0$ (sin 2β)

The measurement of *CP* violation in $B^0 \rightarrow J/\psi K_s^0$ was performed on $1\,\text{fb}^{-1}$ and updated using the whole Run I dataset of $3\,\text{fb}^{-1}$. The effective tagging power increased from $\varepsilon = 2.38\,\%$ $(1\,\text{fb}^{-1})$ [10] to $\varepsilon = 3.02\,\%$ $(3\,\text{fb}^{-1})$ [11]. This increase was mainly due to the use of the SS pion tagger which adds more than $0.376\,\%$ in the newest analysis. As in the measurement of sin 2β the statistical uncertainties are of the order of the systematic uncertainties and the flavour tagging contribution was expected to be a dominant factor an "ad-hoc" calibration was performed. The OS taggers were calibrated with the control channel $B^+ \rightarrow J/\psi K^+$, the SS pion tagger was calibrated with $B^0 \rightarrow J/\psi K^{*0}$. For both decay modes the kinematic variables influencing the calibration needed to be reweighted to the signal decay. Thus using these similar decays with high event yields as control channels allowed to control the size of the systematic uncertainties due to the portability. This approach decreased the size of the systematic uncertainty coming from the flavour tagging calibration to 33 % of the total systematic uncertainty [11].

References

[1] LHCb Collaboration, R.Aaij et. al., *Opposite-side flavour tagging of B mesons at the LHCb experiment, Eur.Phys.J.* C72 (2012) 2022

[2] LHCb Collaboration, R. Aaij et. al., *Optimization and calibration of the same-side kaon tagging algorithm using hadronic B_s^0 decays in 2011 data,* LHCb-CONF-2012-033

[3] G. A. Krocker, *Development and calibration of a same side kaon tagging algorithm and measurement of the $B_s^0 - \bar{B}_s^0$ oscillation frequency Δm_s at the LHCb experiment,* PhD thesis, Heidelberg U., Sep, 2013, CERN-THESIS-2013-213

[4] LHCb Collaboration, R. Aaij et. al., *Measurement of CP violation and the B_s^0 meson decay width difference with $B_s^0 \rightarrow J/\psi K^+ K^-$ and $\bar{B}_s^0 \rightarrow J/\psi \pi^+ \pi^-$ decays,* Phys.Rev. D87 (2013) 11, 112010

[5] LHCb Collaboration, R. Aaij et. al., *Precision measurement of CP violation in $B_s^0 \rightarrow J/\psi K^+ K^-$ decays,* Phys.Rev.Lett. 114 (2015) 4, 041801

[6] LHCb Collaboration, R. Aaij et. al., *Measurement of the CP-violating phase ϕ_s in $\bar{B}_s^0 \rightarrow J/\psi \pi^+ \pi^-$ decays,* Phys.Lett. B713 (2012) 378-386

[7] LHCb Collaboration, R. Aaij et. al., *Measurement of the CP-violating phase ϕ_s in $\bar{B}_s^0 \rightarrow J/\psi \pi^+ \pi^-$ decays,* Phys.Lett. B736 (2014) 186-195

[8] LHCb Collaboration, R. Aaij et. al., *Measurement of the CP-violating phase ϕ_s in $\bar{B}_s^0 \rightarrow D_s^+ D_s^-$ decays,* Phys.Rev.Lett. 113 (2014) 21, 211801

[9] LHCb Collaboration, R. Aaij et. al., *B flavor tagging using reconstructed charm decays at the LHCb experiment,* LHCb-PAPER-2015.027

[10] LHCb Collaboration, R. Aaij et. al., *Measurement of the time-dependent CP asymmetry in $B^0 \rightarrow J/\psi K_s^0$ decays,* Phys.Lett. B721 (2013) 24-31

[11] LHCb Collaboration, R. Aaij et. al., *Measurement of CP violation in $B^0 \rightarrow J/\psi K_s^0$ decays,* Phys.Rev.Lett. 115 (2015) 3, 031601